# Tunable microwave signal generation based on an Opto-DMD processor and a photonic crystal fiber*

Wang Tao(王 涛)[a)†], Sang Xin-Zhu(桑新柱)[a)], Yan Bin-Bin(颜玢玢)[a)], Ai Qi(艾 琪)[b)], Li Yan(李 妍)[a)], Chen Xiao(陈 笑)[b)], Zhang Ying(张 颖)[b)], Chen Gen-Xiang(陈根祥)[b)], Song Fei-Jun(宋菲君)[a)], Zhang Xia(张 霞)[a)], Wang Kui-Ru(王葵如)[a)], Yuan Jin-Hui(苑金辉)[a)], Yu Chong-Xiu(余重秀)[a)], Xiao Feng(肖 峰)[c)], and Alameh Kamal[c)]

[a)] *State Key Laboratory of Information Photonics and Optical Communications, Beijing University of Posts and Telecommunications, Beijing* 100876, *China*
[b)] *College of Science, Minzu University of China, Beijing* 100081, *China*
[c)] *WA Center of Excellence for MicroPhotonic System, Electron Science Research Institute, Edith Cowan University, Joondalup, WA* 6027, *Australia*

(Received 28 September 2013; revised manuscript received 19 November 2013; published online 20 April 2014)

Frequency-tunable microwave signal generation is proposed and experimentally demonstrated with a dual-wavelength single-longitudinal-mode (SLM) erbium-doped fiber ring laser based on a digital Opto-DMD processor and four-wave mixing (FWM) in a high-nonlinear photonic crystal fiber (PCF). The high-nonlinear PCF is employed for the generation of the FWM to obtain stable and uniform dual-wavelength oscillation. Two different short passive sub-ring cavities in the main ring cavity serve as mode filters to make SLM lasing. The two lasing wavelengths are electronically selected by loading different gratings on the Opto-DMD processor controlled with a computer. The wavelength spacing can be smartly adjusted from 0.165 nm to 1.08 nm within a tuning accuracy of 0.055 nm. Two microwave signals at 17.23 GHz and 27.47 GHz are achieved. The stability of the microwave signal is discussed. The system has the ability to generate a 137.36-GHz photonic millimeter signal at room temperature.

**Keywords:** fiber lasers, four-wave mixing, Opto-DMD processor, tunable microwave signal

**PACS:** 42.55.Wd, 42.55.Tv **DOI:** 10.1088/1674-1056/23/6/064217

## 1. Introduction

In recent years, techniques for the optical generation of tunable high-microwave signals have been investigated for many applications, such as broad-band wireless access networks, wireless sensing networks, radio-over-fiber networks, radio over fiber (ROF) systems, software-defined radio, satellite communication, radar, etc. Compared with conventional electronic circuitry means, which are complicated and high loss because of electrical distribution lines, optical generation exhibits excellent advantages, such the ability to generate tunable high-microwave signals, low phase noise, and long-distance transmission in the low cost of fiber. In addition, the optical generation of microwave signals can be assigned to many antenna transmitting terminals. The external modulation technique based on a single-distributed feed back (DFB) laser source and a Mach–Zehnder modulator was employed to generate microwave signals.[1] Based on the polarization-dependent properties of the lithium niobate phase modulator, the 40-GHz microwave signal was achieved using an amplified signal generator and phase modulator with 10-GHz bandwidth.[2] However, high-quality microwave reference source and high-speed modulator were indispensable. Optical generation of microwave signals by the optical heterodyning technique was presented.[3–8] The high quality microwave reference source was necessary to ensure phase stabilization. Generation of a microwave signal using a dual-wavelength single-longitudinal-mode (SLM) fiber ring laser was realized by utilizing dual-wavelength ultra-narrow transmission-band fiber Bragg grating (FBGs).[9] The microwave signal at 20.07 GHz with a line-width less than 25 kHz was demonstrated by incorporating a delay interferometer (DI).[10] However, due to the limitation of the wavelength spacing, the microwave frequency was only above 20.07 GHz.

Tunable fiber lasers were demonstrated based on tunable fiber-Bragg-grating, liquid crystal opto-very-large-scale-integrated (VLSI)[11,12] and tunable polarization maintaining fiber (PMF) Lyot–Sagnac filter.[13] Recently, we realized a stable dual-wavelength tunable laser based on liquid crystal opto-VLSI and four wave-mixing in the high nonlinear photonic crystal fiber.[11] Here, the optical generation of a tunable microwave signal is demonstrated with an opto-digital-micromirror-device (Opto-DMD) processor and photonic crystal fiber. The high-nonlinear photonic crystal fiber (PCF) is employed for the generation of the four-wave mixing (FWM) to obtain stable and uniform dual-wavelength oscillation. Two different short passive sub-ring cavities, which

*Project supported by the National Basic Research Program of China (Grant No. 2010CB327605), the Specialized Research Fund for the Doctoral Program of Higher Education, China (Grant No. 20120005120021), the Fundamental Research Funds for the Central Universities, China (Grant No. 2013RC1202), the Program for New Century Excellent Talents in University, China (Grant No. NECT-11-0596), and the Beijing Nova Program, China (Grant No. 2011066).

†Corresponding author. E-mail: tomwangbupt@163.com

© 2014 Chinese Physical Society and IOP Publishing Ltd 

are inserted into the main ring cavity, serve as mode filters to make SLM lasing. The tunable microwave signals are obtained by beating two lasing wavelengths at a high-speed photodetector (PD). The two lasing wavelengths are easily electronically selected by loading different gratings on an Opto-DMD processor controlled with a computer. Hence, the target of smartly tuning the generated microwave frequency, which corresponds to the wavelength spacing between two lasing wavelengths, can be achieved easily by flexibly changing the wavelength spacing. The wavelength spacing can be experimentally tuned from 0.165 nm to 1.08 nm within a tuning accuracy of 0.055 nm, and the frequency can be tuned from 17.5 GHz to 135 GHz.

## 2. Experimental setup and analysis

Figure 1 shows the schematic configuration of the experimental system for generating the tunable microwave signals. An erbium-doped fiber amplifier (EDFA), an Opto-DMD processor, two sections of single-mode optical fiber with different lengths, a 30-m-long high-nonlinear PCF and a 1200-$mm^{-1}$ blazed grating plate, are used. The fiber in the EDFA is employed as the gain medium. The Opto-DMD processor consists of 1024 × 768 pixels controlled by a micro-electro-mechanical element. A two-dimensional (2D) blazed grating can be generated, and any two wavelengths of the ASE spectra can be steered by uploading the corresponding voltage on the appropriate mirrors. The polarization controller (PC) ensures that the system will generate the single lasing polarization, and optimize the diffraction efficiency of the Opto-DMD processor. The collimator array transforms the divergent beam into collimated light, so that the coupling loss is reduced. The 1200-$mm^{-1}$ blazed grating plate is an amplified spontaneous emission (ASE) demultiplexer, and the blazed angle is 70°. The 1×2 coupler with a 10:90 power splitting ratio splits the light from the erbium-doped fiber amplifier (EDFA), where 10% of the power is used to extract the laser output while 90% of the power is re-circulated in the main fiber ring. The Opto-DMD can generate a 2D blazed grating by correspondingly driving, and the diffraction effect is obvious in the near infrared band. Two optical couplers connect to the fibers with different lengths, and constitute the sub-ring. The high-nonlinear PCF is inserted into the main fiber ring, with a nonlinear coefficient of $\sim 11$ $W^{-1}\cdot km^{-1}$ and a flat dispersion of $\sim 1$ ps/(nm/km) around 1550 nm. The 1200-$mm^{-1}$ blazed grating plate with a shining angle of 70° at 1530 nm, is employed to demultiplex the ASE spectrum and generate lasing window onto the surface of the Opto-DMD processor. The output laser is split into two parts by another 10:90 1×2 optical coupler, 90% of the output power is applied to the high-speed PD while the 10% part is monitored by an optical spectrum analyzer (OSA). The optical generated microwave signal is observed by an electrical spectrum analyzer (ESA).

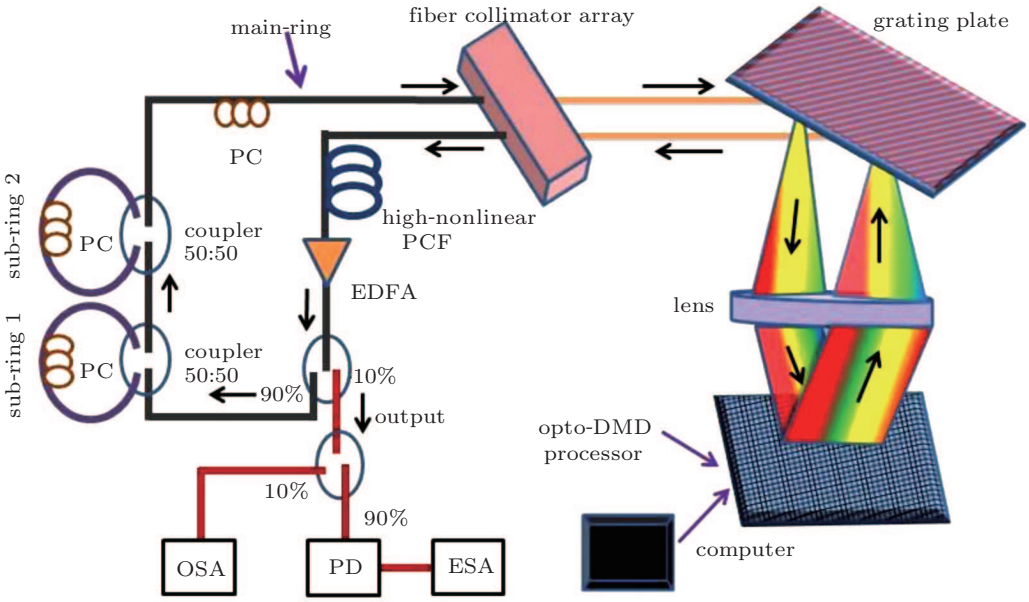



**Fig. 1.** (color online) Experimental setup. DMD: digital micro-mirror devices, PC: polarization controller, OSA: optical spectrum analyzer, PD: photodetector, ESA: electrical spectrum analyzer, PCF: photonic crystal fiber.

In the experimental setup, the core component is the Opto-DMD (0.55″ DMD) processor.[14] It is a semiconductor-based 1024 pixel ×768 pixel array of addressable mirror-pixels, and the side length of pixel is 10.8 μm. The Opto-DMD processor is actually a semiconductor optical switch that million square micro-mirrors are integrated in the com-

plementary metal–oxide–semiconductor (CMOS) silicon substrate. Each micro-mirror represents a pixel and can independently rotate $\pm 12^{\circ}$ along its diagonal direction by using a similar hinge effect of rotating device at the bottom. The corresponding part of the ASE spectrum of EDFA mapping onto the different rectangular tilting pixel blocks can diffract efficiently by uploading the corresponding voltage on the appropriate mirrors. Because the voltage is only applied to the selected pixel address when the system is running, the next corresponding mirror could be tilted. The rest of the ASE spectrum of EDFA is directly reflecting on the unselected pixels, and this part of the light will not be coupled into the optical fiber collimator. Finally, it can achieve the target that the selected wavelengths of light are gaining and other wavelengths are attenuating. 90% of the ASE light generated by the EDFA is coupled to the blazed grating plate through one port of the dual fiber collimator. The dispersion appears in the first-order diffraction direction. The dispersed light is mapped onto different rectangular pixel blocks of the Opto-DMD processor. The Opto-DMD processor can arbitrarily select dual-wavelength from the ASE spectrum of the EDFA with two different steering gratings generated on the Opto-DMD processor, which is coupled back into the other port of the collimator and amplified by the EDFA. However, the dual-wavelength is extremely unstable and non-uniform due to the homogeneous gain broadening of the erbium-doped fiber (EDF). As the high-nonlinear PCF is inserted into the laser cavity, the FWM effect can suppress the mode competition and the homogeneous gain broadening.[11] The dual-wavelength light beams are amplified by the EDFA and repeatedly re-circulated through the main cavity. Two sub-ring cavities can select a longitudinal-mode according to the central wavelength. A stable and tunable SLM dual-wavelength can be achieved. The light field of two lasing beams can be expressed as[15]

$$E_1 = A_0 \cos(\omega_1 t + \varphi_1), \quad E_2 = A_0 \cos(\omega_2 t + \varphi_2), \tag{1}$$

where

$$\varphi_1 = -\frac{2\pi}{\lambda}\Delta L_1 + \varphi_{10}, \quad \varphi_2 = -\frac{2\pi}{\lambda}\Delta L_2 + \varphi_{20},$$

with $\Delta L_1$ and $\Delta L_2$ being the optical path differences, $\varphi_{10}$ and $\varphi_{20}$ being the initial phases. The total intensity is

$$\begin{aligned} I &= (E_1 + E_2)^2 \\ &= A^2 [\cos(\omega_1 t + \varphi_1) + \cos(\omega_2 t + \varphi_2)]^2 \\ &= A^2 \{1 + \cos[(\omega_1 - \omega_2)t + (\varphi_1 - \varphi_2)] \\ &\quad + \cos[(\omega_1 + \omega_2)t + (\varphi_1 + \varphi_2)] \\ &\quad \times (1/2)\cos(2\omega_1 t + 2\varphi_1) + (1/2)\cos(2\omega_2 t + 2\varphi_2)\}. \end{aligned} \tag{2}$$

Compared with the light frequency $f_{\text{light}}$, the cut-off response frequency $f_{\text{PD}}$ of PD is small enough, and the items $\omega_1 + \omega_2$, $2\omega_1$, and $2\omega_2$ can be omitted. Equation (2) can be simplified into

$$\begin{aligned} I &= A^2 \cos[(\omega_1 - \omega_2)t + (\varphi_1 - \varphi_2)] \\ &= A^2 \cos\left[(\omega_1 - \omega_2)t + \frac{2\pi}{\lambda}(\Delta L_2 - \Delta L_1) + (\varphi_{10} - \varphi_{20})\right], \end{aligned} \tag{3}$$

where $\omega_1 - \omega_2$ is the so-called beat frequency. Based on the condition $f_{\text{PD}} = f_{\text{light}}$, the approximate response of PD can be written as

$$\begin{aligned} I &\approx \frac{A^2}{T}\int_0^T \cos\left[(\omega_1 - \omega_2)t + \frac{2\pi}{\lambda}(\Delta L_2 - \Delta L_1) + (\varphi_{10} - \varphi_{20})\right] \mathrm{d}t \\ &\approx A^2 \sin\left[(\omega_1 - \omega_2)T + \frac{2\pi}{\lambda}(\Delta L_2 - \Delta L_1) + (\varphi_{10} - \varphi_{20})\right]. \end{aligned} \tag{4}$$

To generate microwave signals by the optical heterodyning technique, the two lasing beams from the output of only a single laser source should satisfy several conditions. Firstly, the phase fluctuations should be as small as possible. Secondly, the wavelength difference between two lasing beams should keep stable, and the two lasing wavelengths must be oscillating SLM. Since the microwave signals are generated with only a single laser source, two lasing wavelengths share the same gain medium EDF in the laser ring cavity, the phase fluctuations can be minimized as much as possible.

By applying two different appropriate steering gratings to the Opto-DMD processor without any mechanical shift, the arbitrary two lasing wavelengths can be independently and reliably steered and coupled into the fiber collimator. Suppose that two beams are selected to be lasing at $\lambda_1$ and $\lambda_2$ (corresponding to two frequencies $\omega_1$ and $\omega_2$). The mode competition caused by the EDF as a homogeneous medium is detrimental to the output of a uniform dual-wavelength. In order to make the two lasing beams stable and uniform, the high-nonlinear PCF, which causes two degenerate FWM processes, is inserted into the main cavity. The basic principle of inhibiting mode competition by FWM is to compensate for the optical powers of different wavelengths through the redistribution of beam energies.[11,16] The two degenerate FWM processes, namely $\omega_2 + \omega_3 = 2\omega_1$ and $\omega_1 + \omega_4 = 2\omega_2$, can generate another two wavelengths $\omega_3$ and $\omega_4$. Here, we define $P_1$, $P_2$, $P_3$, and $P_4$ as the optical powers at the frequencies $\omega_1$, $\omega_2$, $\omega_3$, and $\omega_4$, respectively, and they can be related by[17]

$$P_3 = \gamma^2 L^2 P_1^2 P_2, \tag{5}$$

$$P_4 = \gamma^2 L^2 P_2^2 P_1. \tag{6}$$

Here, parameter $\gamma$ represents the nonlinear coefficient of the fiber, $L$ is the interaction length of FWM. The corresponding increments of powers at $\omega_1$ and $\omega_2$, namely $\Delta P_1$ and $\Delta P_2$, originate from $\omega_2$ and $\omega_1$, respectively. In our experiment, two photons of frequency $\omega_1$ are annihilated to produce one photon of frequency $\omega_3$ and other photon of frequency $\omega_2$, and

$\omega_3 \approx \omega_2$, so $\Delta P_2$ can be determined as

$$\Delta P_2 \approx P_3 = \gamma^2 L^2 P_1^2 P_2. \quad (7)$$

A similar procedure plays the same role in valuing $\Delta P_1$

$$\Delta P_1 \approx P_4 = \gamma^2 L^2 P_2^2 P_1. \quad (8)$$

As a conclusion, the difference $\Delta P$ between $\Delta P_1$ and $\Delta P_2$ can be determined as

$$\Delta P = \Delta P_1 - \Delta P_2 = \gamma^2 L^2 P_1 P_2 (P_2 - P_1). \quad (9)$$

Therefore, when $P_2 > P_1$, then $\Delta P > 0$, so the energies are transferred from $\omega_2$ to $\omega_1$, when $P_2 < P_1$, then $\Delta P < 0$, the energies are transferred from $\omega_1$ to $\omega_2$. Under the action of two degenerate FWMs, the two lasing beams become stable and uniform at room temperature.

The Opto-DMD not only selects the output wavelength, but also serves as a mode restriction element to provide the preliminary selection of laser modes. However, the bandwidth of the Opto-DMD filter is relatively wide, and the further mode selection should be provided by two sub-rings. Two passive sub-rings are inserted into the main cavity to serve as a single-longitudinal-mode filter.[18,19] According to the Vernier effect,[20] the oscillating mode of EDFL with sub-ring cavities should simultaneously satisfy the resonant conditions of both the main ring cavity and two sub-ring cavities. According to the basic principle of the ring laser, the resonant mode condition, which includes the main ring and the subring, can be described by

$$\beta L_{\text{main}} = 2m\pi, \quad (10)$$

$$\beta L_{\text{sub}} = (2n+1)\pi, \quad (11)$$

where sub$= 1, 2$, $L_{\text{main}}$ is the length of the main cavity, $L_{\text{sub}}$ is the length of the two sub-ring cavities, respectively. $\beta$ is the propagation constant, $m$ and $n$ are all positive integers. In the case of satisfying the phase condition of both the main cavity and two sub-ring cavities at the same time, the laser mode only can oscillate. The free spectral range (FSR) of the ring cavity can be described by[19]

$$\text{FSR}_{\text{main}} = c/nL_{\text{main}}, \quad (12)$$

$$\text{FSR}_{\text{sub}} = c/nL_{\text{sub}}, \quad (13)$$

where $c$ is the speed of light in a vacuum, $n$ is the effective refractive index of the fiber loop, $\text{FSR}_{\text{main}}$ is the FSR of the main ring cavity, and $\text{FSR}_{\text{sub}}$ is the FSR of the sub-ring cavity. Generally, each ring resonator has its own resonant frequency. The $\text{FSR}_{\text{MRC}}$ of the MRC laser should take the least common multiple of $\text{FSR}_{\text{MRC}}$ and $\text{FSR}_{\text{sub}}$,

$$\text{FSR}_{\text{MRC}} = 2m\text{FSR}_{\text{main}} = (2n+1)\text{FSR}_{\text{sub}} = (\text{FSR}_{\text{main}}, \text{FSR}_{\text{sub1}}, \text{FSR}_{\text{sub2}})_{lcm}. \quad (14)$$

The $\text{FSR}_{\text{MRC}}$ of the SLM laser will become so large that it can suppress the other longitudinal-modes to achieve SLM.

## 3. Experimental results and discussion

The output laser wavelength shifts 0.055 nm while one pixel in the Opto-DMD is changed (i.e., 0.055 nm/pixel), under computer controlling, and the corresponding frequency bandwidth at 1550 nm is 6.87 GHz. In order to obtain dual-wavelength SLM lasing, two sub-ring cavities are inserted into the main cavity. In order to compare the difference between SLM lasing operation and MLM lasing operation, the corresponding result is shown in Fig. 2 before two sub-ring cavities are used. It can be seen that the laser operates in MLM. When the main cavity is combined with two sub-ring cavities, mode competition will be well suppressed. The lengths of sub-rings are 1.9 m and 2.1 m, corresponding to the FSRs of nearly 107.56 MHz and 97.31 MHz, respectively. According to the Vernier effect, the FSR can be above 41.5 GHz, which is larger than the filter bandwidth. In this way, SLM dual-wavelength lasing can be achieved.

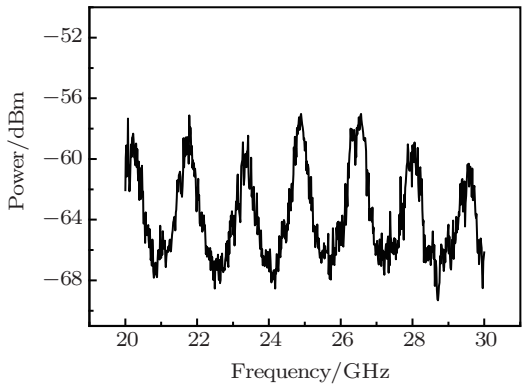



**Fig. 2.** Output electrical spectrum in MLM operating with only the main ring.

As shown in Fig. 3, the stable dual wavelength SLM laser is achieved with the influence of the FWM process in the high-nonlinear PCF. Figure 3(a) shows that the dual-wavelength lasing with an interval between the two steering gratings on the Opto-DMD processor of 3 pixels. It is detected by a high-speed 30-GHz PD (u2t photonics The Optilab PD-30 GHz), and a 17.23-GHz beat signal is achieved. The electrical spectrum of the beat signal is measured by an ESA (R&S FSV-30 GHz) as shown in Fig. 4(a). We can see that only a microwave signal can be observed, which means that the dual-wavelength laser is operating in SLM. When we adjust the interval between two steering gratings to 4 pixels, the output optical spectrum and the microwave spectrum are given in Figs. 3(b) and 4(b) respectively. A 27.47-GHz optical microwave signal is generated.

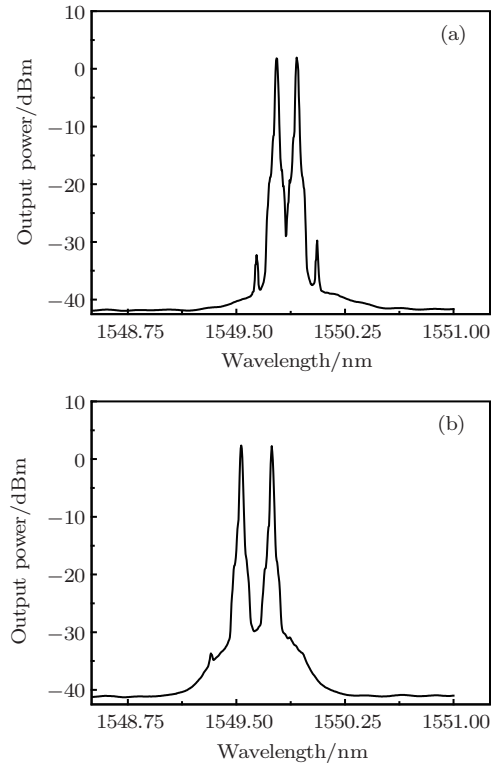



**Fig. 3.** Output spectra of the dual-wavelength SLM lasing, with wavelength spacings being (a) 3 pixels and (b) 4 pixels.

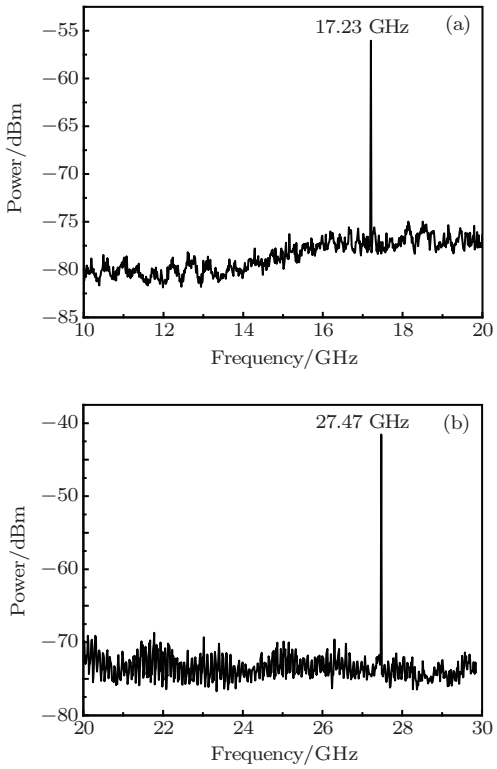



**Fig. 4.** Output electrical spectra of optical microwave signal when two sub-ring cavities are inserted, showing (a) 17.23-GHz microwave signal corresponding to an interval of 3 pixels, and (b) 27.47-GHz microwave signal corresponding to an interval of 4 pixels.

Figure 5 shows that the power fluctuation of the 17.23-GHz microwave signal is 8.9 dB, and the power fluctuation of the 27.47-GHz microwave signal is below 2 dB. The stability of the microwave signal at 27.47 GHz generated with a 4-pixel spacing is improved. When the interval between two steering gratings is 3 pixels, the corresponding theoretical wavelength spacing is 0.165 nm, while the measured wavelength spacing is 0.14 nm. When the interval of 4 pixels is used, the corresponding theoretical wavelength spacing is 0.21 nm, which is close to the measured result.

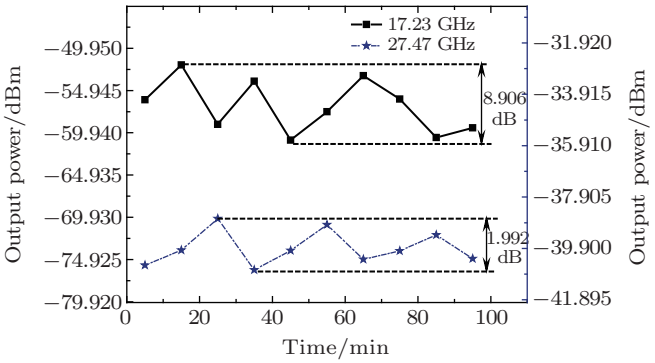



**Fig. 5.** (color online) Power fluctuations when microwave signals at 17.23 GHz and 27.47 GHz, respectively.

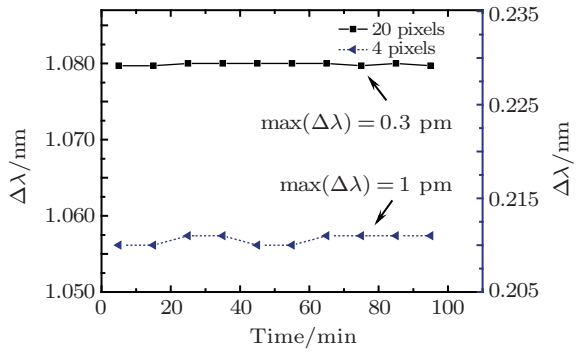



**Fig. 6.** (color online) Fluctuations of wavelength with the intervals of 4 pixels and 20 pixels.

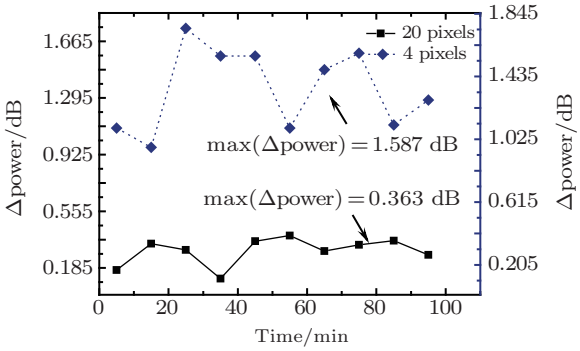



**Fig. 7.** (color online) Fluctuations of power difference with the intervals of 4 pixels and 20 pixels.

With the increase of the interval between the two steering gratings, fluctuations on the power and the wavelength difference decrease, which indicates that the stability of the generated microwave signal is improved. Fluctuations on wavelength and power difference are shown in Figs. 6 and 7. When the interval is 20 pixels, the maximum fluctuations on power and wavelength difference are 0.363 dB and 0.3 pm respectively, and the spectra in the 150 min are shown in Fig. 8.

The side-mode suppression ratio is 45 dB and the wavelength spacing is 1.08 nm, which shows that a stable 137.36-GHz photonic millimeter signal can be generated.

The tunable capability of a photonic microwave signal can be smartly achieved based on the tunable wavelength spacing by controlling the interval between the two reconfigurable steering gratings. The output spectra of the dual-wavelength SLM lasing with different intervals are shown in Fig. 9. When the interval is 1 pixel or 2 pixels, the mode competition between two SLM wavelengths is too serious to guarantee the stable dual-wavelength laser. The unstable SLM dual-wavelength laser is adverse to the generation of an optical microwave signal. When the interval is above 2 pixels, a stable microwave signal can be generated. The relations of wavelength spacing and microwave frequency to interval are shown in Figs. 10(a) and 10(b) respectively. The generated optical microwave signal frequency can range from 17.23 GHz to 137.36 GHz. Due to the limitation of the cut-off frequency of our available PD and ESA, the highest measured frequency for the microwave signal is 27.47 GHz.

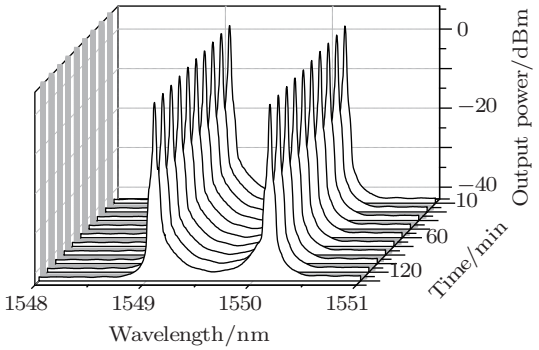



**Fig. 8.** Measured output spectrum of the SLM dual-wavelength laser for 150 min when the wavelength spacing is 20 pixels.

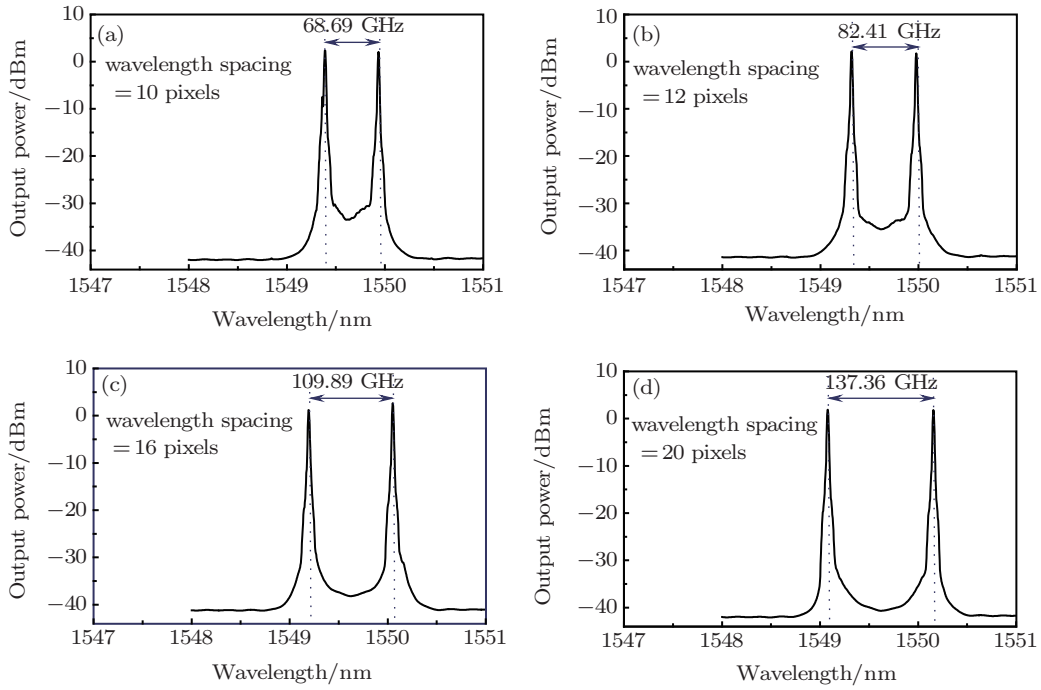



**Fig. 9.** Output spectra of the dual-wavelength SLM lasing with intervals of (a) 10, (b) 12, (c) 16, and (d) 20 pixels.

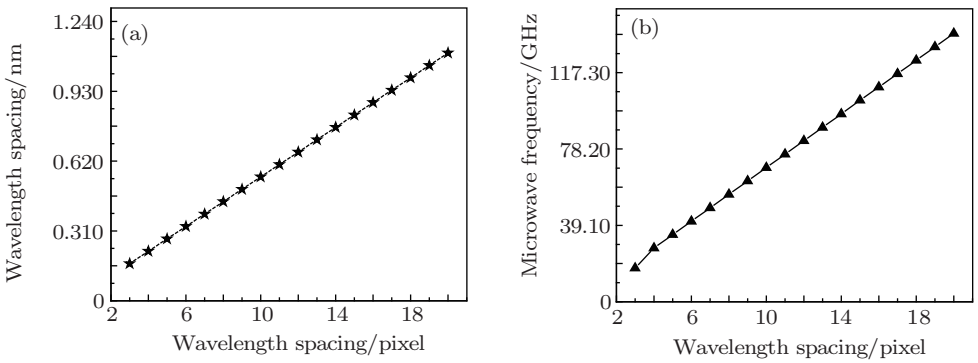



**Fig. 10.** (a) Wavelength spacing and (b) optical microwave frequency versus interval.

## 4. Conclusions

In this paper, the frequency-tunable microwave signal generation is experimentally demonstrated with a dual-wavelength SLM erbium-doped fiber ring laser based on a digital Opto-DMD processor and FWM in a high-nonlinear PCF. The two lasing wavelengths are electronically selected by loading different reconfigurable gratings on the Opto-DMD processor. The high-nonlinear PCF is employed for the generation of the FWM to obtain stable and uniform dual-wavelength oscillation. The two sub-ring cavities can suppress the mode competition and ensure that the dual-wavelength oscillates in SLM. The wavelength spacing can be smartly adjusted from 0.165 nm to 1.08 nm within a tuning accuracy of 0.055 nm. Two microwave signals at 17.23 GHz and 27.47 GHz are obtained by beating the SLM dual-wavelength at a PD. The stability of microwave signals is discussed. The system has the ability to generate a 137.36-GHz photonic millimeter signal.

## References


[1] O'Reilly J J, Lane P M, Heidemann R and Hofstertt R 1992 *Electron. Lett.* **28** 2309

[2] Hedekvist P O, Olsson B E and Wiberg A 2004 *Journal of Lightwave Technology* **22** 882

[3] GlieseU, Nielsen T N, Bruun M, Christensen E L, Stubkjaer K E, Lindgren S and Broberg B 1992 *IEEE Photon. Technol. Lett.* **4** 936

[4] Bordonaalli A C, Walton C and Seeds A 1999 *Journal of Lightwave Technology* **17** 328

[5] Genest J, Chamberl M, Tremblay P and Tetu M 1997 *IEEE J. Quantum Electron.* **33** 989

[6] Fan Z and Dagenais M 1997 *IEEE Trans. Microwave Theory Technol.* **45** 1296

[7] Goldberg L, Taylor H F, Weller J F and Bloom D M 1983 *Electron. Lett.* **19** 491

[8] Williams K J, Goldberg L, Esman R D, Dagenais M and Weller J F 1989 *Electron. Lett.* **25** 1242

[9] Chen X F, Deng Z C and Yao J P 2006 *IEEE Trans. Microwave Theroy Technol.* **54** 804

[10] Chen G J, Huang D X, Zhang X L and Cao H 2008 *Opt. Lett.* **33** 554

[11] Peng L, Sang X Z, Yan B B, Chen X, Wang Y, Zhang Y, Xiao F and Alameh K 2012 *Opt. Laser Technol.* **44** 935

[12] Xiao F, Alameh K and Lee S 2009 *Opt. Express* **17** 18676

[13] Wang W, Meng H, Wu X, Xue H, Tan C and Huang X 2012 *IEEE Photon. Technol. Lett.* **24** 470

[14] Dana D, Walter M D and John S 2003 *SPIE*, January 20, 2003, San Jose, CA, USA, p. 4985

[15] Tang J X 1990 "Optical Beat and Interference" *College Phys.* p. 10

[16] Wang H Y and Xu X S 2013 *Chin. Phys. B* **22** 054205

[17] Liu X M, Zhou X Q and Lu C 2005 *Opt. Lett.* **30** 2257

[18] Feng T, Yan F P, Li Q, Peng W J, Feng S C, Tan S Y and Wen X D 2013 *Chin. Phys. B* **22** 014208

[19] Lee C C, Chen Y K and Liaw S K 1998 *Opt. Lett.* **23** 358

[20] Onodera N 1997 *Electron. Lett.* **33** 962